GNC challenges for SIMBOL-X formation flying mission

P. Y Guidotti, M. Delpech, S. Djalal, A. Gaudel-Vacaresse, J. C. Berges, P. Gamet, Olivier La Marle

Abstract

SIMBOL-X is a hard X-ray space-based observatory to be launched in 2013 onto a High Elliptical Orbit (HEO). This new generation telescope covers by a single instrument a continuous energy range starting at classical X-rays and extending to hard X-rays (i.e. from 0.5 to 80 keV). For mass and size reasons, a classical monolithic instrument cannot be used and this Franco-Italian mission will thus consist of two satellites. The Mirror spacecraft (MSC) will be in free flight on a HEO orbit and will target very precisely the source to observe, focusing the hard X-ray emission thanks to its mirror module. At the focal point, 20 meters behind the Mirror satellite, the Detector spacecraft (DSC) maintains its position on a forced orbit. This paper aims at presenting some of SIMBOL-X GNC challenges. The first part will introduce main formation flying phases and related system requirements. In the next section focus will be made on DSC GNC design: algorithms and equipment adapted to the previously introduced phases will be presented. The last section deals with the line-of-sight (LOS) restitution problematic: for scientific purposes the line-of-sight between the two spacecrafts shall be reconstructed a posteriori very precisely. The last section will thus describe the chosen methodology to address this challenging problem.

1. Mission overview

1.1. SIMBOL-X mission

SIMBOL-X mission aims mainly at understanding black hole physics and acceleration mechanisms. It will also cover other challenging aspects in the domain of high-energy astrophysics and cosmology, such as the formation of stars and planets for example. In the hard X-ray domain, SIMBOL-X mission will provide a sensitivity and an angular resolution comparable to the best ones obtained so far in soft X-ray. The SIMBOL–X telescope relies on a mirror module based on multilayer coated shells used in grazing incidence in the Wolter-I optimal configuration and on a detector payload located in the mirror focal plane. The trade-off between the size of the field of view and the effective area at high energies led to an optimized 20 m focal length. The size of space-based monolithic telescopes is limited by the performances of the available launchers. To

overcome this difficulty the instrument is thus separated in a mirror and a detector flying in formation (Fig. 1). Very high performances are reached with an overall mass and size far much lower than with an equivalent monolithic observatory : Simbol-X overall launch mass does not exceed 1900 kg (811 kg for the detector satellite and 1056 kg for the mirror satellite).

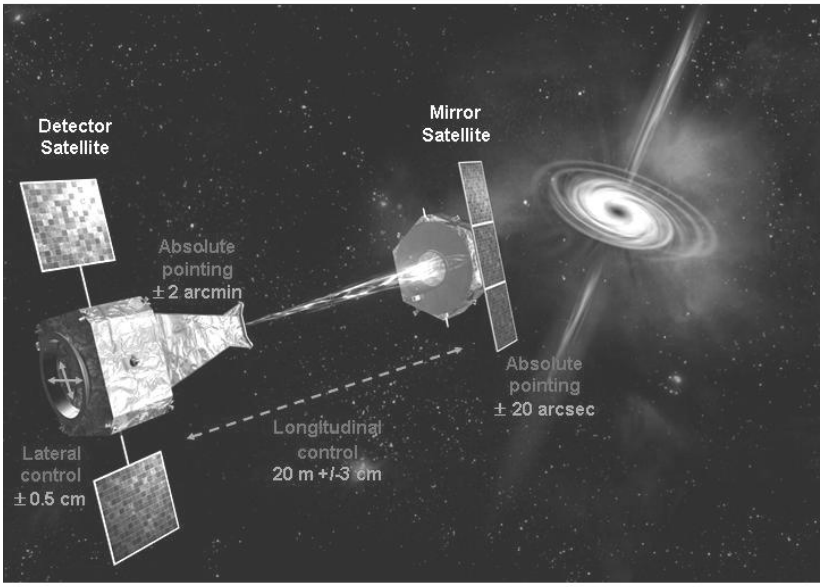

Fig. 1 SIMBOL-X formation during observations

The SIMBOL-X project is a cooperation between the French Space Agency (CNES) and the Italian Space Agency (ASI). The design of the instrument involves a number of laboratories in France (CEA, CESR, APC), in Italy (INAF, IASF) and in Germany (MPE, IAAT, TUD).

1.2. Mission phases

The scientific mission accomplishment relies first of all on the correct acquisition of the observation configuration. This observation configuration depends on the correct formation acquisition first and then on the correct formation control accuracy. As previously explained, when observing a source the Detector spacecraft shall be maintained 20 m behind the Mirror spacecraft. But after launcher separation and during the whole Station keeping phase the two spacecrafts are controlled and monitored independently from the ground: they may be separated by tenths of kilometers. An incremental approach is thus needed in order to reduce the intersatellite distance and switch the formation control from the ground to the board, guaranteeing by this way the first step towards observation configuration. This incremental approach leads to different needs regarding phases length and autonomy. The mission phases, presented on Fig. 2, are thus described briefly before focusing on the specific formation acquisition sequence.

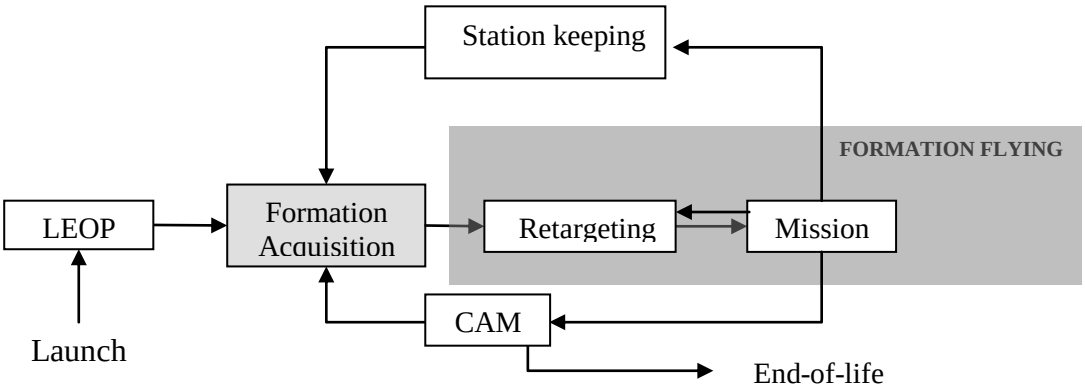

Fig. 2 SIMBOL-X mission phases

After the separation from the launcher, during the Low Earth Orbit Phase (LEOP), the two spacecrafts are set onto their reference orbit, in a safe configuration, using ground computed maneuvers. Currently the relative configuration of the spacecrafts is still under evaluation: a difference in eccentricity will lead to in-plane relative motion while a difference in inclination will create out-of-plane relative motion too. Regarding anomaly, a difference on this orbital parameter will center DSC relative motion around a virtual point ahead or behind MSC. The choice on this relative configuration will mainly depend on orbit determination accuracy and maneuver realization performances. Another aspect to take into account is the modes commonality: as far as possible, the chosen relative configuration shall be achievable from LEOP phase, from the end of Station keeping and after a Collision Avoidance Maneuver (CAM).

At the end of LEOP phase the distance between the two satellites is of 30 km at the apogee. This is the maximal distance at which the relative metrology based on a Formation Flying Radio Frequency (FFRF) sensor can be activated and validated. Besides the relative dynamics is more favorable in terms of delta-V consumption when reducing the intersatellite distance. Once this coarse metrology has been validated from the ground, the transition from free flying to formation flying phases is thus initiated trough the Formation Acquisition sequence that lasts less than 24 hours. During this sequence, which is detailed further, the Detector satellite approaches autonomously the Mirror satellite reducing the intersatellite distance from 30 km to about 20 m only using on-board FFRF sensor measurements and hydrazine thrusters. The two spacecrafts are already flying in formation but the metrology and the propulsion subsystem are not accurate enough in order to control the relative state with the required performance for scientific observations: the spacecrafts are flying in coarse formation. In order to enter the observation configuration and thus the Mission phase, another equipment set shall be involved: a fine Formation Flying Optical Sensor (FFOS) for the relative metrology and cold gas thrusters for the propulsion subsystem. This

transition is performed during a first Retargeting phase, which is also adapted to the transition between two different observations. This Retargeting phase consists of a reorientation of the whole formation in order to point the telescope to a new target. The system shall be able to perform 1000 instrument retargeting maneuvers during nominal mission, which reduces this phase to 45 minutes. The formation may be broken for Station keeping purposes or after an anomaly occurrence followed by a CAM. After a Station keeping phase or a CAM, another Formation Acquisition sequence is needed to recover the mission.

1.3. Focus on Formation Acquisition phase

During Formation Acquisition phase, the intersatellite distance (ISD) initially around 30 km, shall be safely reduced to tenth of meters in less than 24 hours. The Detector spacecraft shall be able to accurately estimate its relative state with respect to the Mirror spacecraft so that autonomous Rendezvous and closing manoeuvres can be performed. The sequence of the formation acquisition and the ISD associated to each step is given on the diagram below:

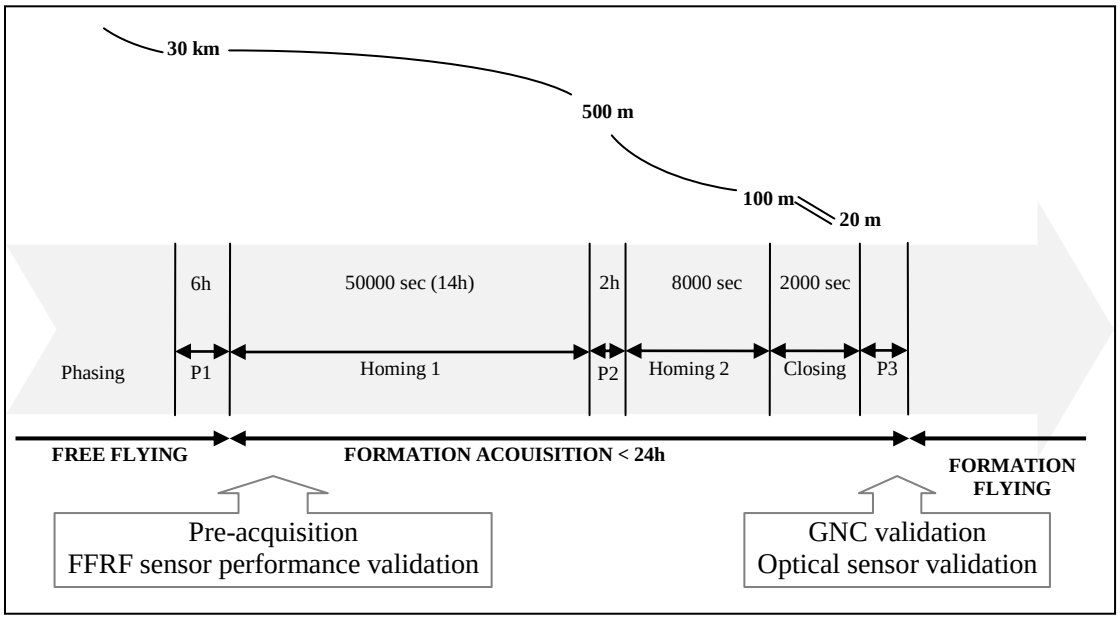

Fig. 3 Formation acquisition sequence

This Point 1 (P1) step corresponds to the transition from the LEOP phase to the Homing phase. The relative motion of the spacecrafts is not controlled. The relative state configuration and knowledge accuracy depend on LEOP operations performance. In order to activate the FFRF sensor which measures the relative distance and the two LOS angles between the two spacecrafts, the nominal ISD is 30 km and the alignment between the two spacecrafts shall be under 20°. The FFRF sensor shall perform an Integer Ambiguity Resolution (IAR) in order to provide fine measurements.

Once the metrology has been validated from ground, the on-board loop can be closed using the FFRF sensor measurements.

During both Homing phases (Homing1 and Homing 2) the on-board relative navigation function provides relative state estimates to the Rendezvous algorithm using FFRF sensor measurements. This relative positioning guidance algorithm computes the maneuvers to be applied on the Detector spacecraft to reduce the ISD to 100 m. An holding point at 500 m is planned in order to perform ground monitoring : it is the Point 2 (P2) step. Rendezvous algorithms do not fix the relative trajectory between the departure point and the arrival point.

At closest ISD, from 100m to approximately 20 m, the relative trajectory needs to be secured. During the Closing sub-phase, the relative positioning guidance is thus a forced translation inside a corridor.

At the end of the Closing sub-phase the ISD is thus short enough to enter the fine relative metrology operating domain. The Point 3 (P3) step enables a validation of the fine relative metrology before its introduction in the on-board GNC loop. The formation is ready to perform a Retargeting in order to point the source commanded from ground and enter the Mission phase.

2. DSC GNC design

After this brief formation flying phases description, focus is made on DSC GNC design in this section. More details are given on algorithms and equipments adapted to the previously introduced phases.

2.1. Relative state concerns

2.1.1. Relative dynamics model

SIMBOL-X reference orbit is a 4-day period orbit (perigee at 20000 km and apogee at 180000 km). This choice enables the spacecrafts to fly above Van Allen belts (73000 km) 83% fraction of the time, so that continuous observations from 0 up to 3.5 days are possible. During most of the orbit, the major disturbance is the solar pressure force. The gravity gradient becomes predominant only at perigee, which also corresponds to the orbit section were no observations are planned (strong radiations below Van Allen belts). Both aspects could eventually lead to widen the position relative control corridor around perigee passes. For relative control and relative navigation design, a rather simple relative dynamics model can be written considering the satellites as free flying objects submitted to slowly varying perturbations. For Formation acquisition relative guidance purposes though, where a propagation of the relative dynamics is needed, a more complex model such as Yamanaka-Ankersen equations [4] is needed to describe the relative motion.

2.1.2. Relative navigation function

The relative navigation algorithm envisioned for SIMBOL-X during all Formation Flying phases, relies on a dynamic filter. Due to non linearities in the observation equation (distance and/or line-of-sight for both FFRF and FFOS sensors) an Extended Kalman Filter is used. Because of the high orbit context the estimation of the perturbing forces is also included in the estimated state. The filter state vector (at least 9 variables) comprises the Detector satellite relative position and velocity w.r.t. Mirror satellite as well as the magnitude of the perturbation (that includes the slowly varying gravity terms).

The relative navigation function relies on a FFRF sensor for coarse formation phases.

The FFRF metrology shown on Fig. 4 FFRF metrologyprovides the relative line-of-sight with an accuracy of 1° (3σ) and the relative distance with an accuracy of 1 cm (3σ) up to 30 km at least.

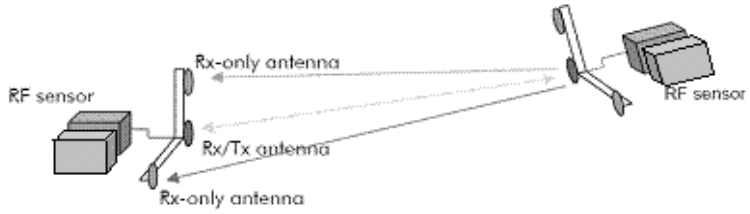

Fig. 4 FFRF metrology

An antenna triplet is mounted on each satellite. This triplet is composed of one Rx/Tx antenna (emitting and receiving) and two Rx antennas. The emitting antennas of each satellite emits alternatively a S-band signal, that is received by the triplet of the other satellite. After processing of the signals phases and code the sensor provides the distance and the line-of-sight of the other satellite.

An omni-directional coverage can be guaranteed by the accommodation of the FFRF sensor on each satellite: in addition to the triplet other antennas shall be placed on the different spacecrafts faces. The omni-directional coverage and the great range of the FFRF metrology, together with its accuracy, makes it the privileged relative metrology sensor during the Formation Acquisition phase and for anti-collision monitoring during all phases. The sensor bias may be included in the filter estimates and the achieved accuracy in position estimation is centimetric.

But for the Mission phase the relative navigation filter relies on the FFOS optical sensor that is presented in Fig. 5. The concept presented here is issued from a Sodern concept [5] (based on a CNES Research and Technology study). It also provides the LOS angles and the relative distance but with 1-arcsec (3σ) accuracy for the LOS and with 1-cm (3σ) accuracy for the relative distance.

On the contrary to FFRF metrology the optical sensor provides this accuracy as soon as it is activated (no special procedure is needed) but its operating domain is obviously much smaller (3° field of view, intersatellite distance less than 25 m).

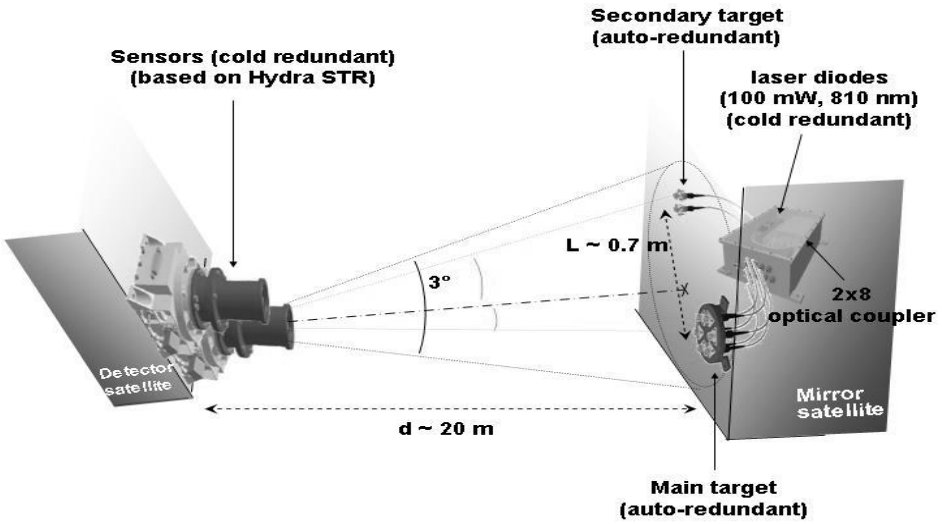

Fig. 5 FFOS metrology based on a Sodern R&T study

This optical sensor is composed of an optical head mounted on the DSC and based on Sodern Hydra star-tracker technology. On the MSC two active targets are facing the optical head: the main target processing provides the LOS angles while the inter-satellite range is obtained from the secondary target processing, knowing the targets geometry. Regarding bias, a cumulated bias calibration (thus including FFOS bias) is foreseen with the scientific payload. The achieved accuracy in lateral position estimation is finally millimetric.

2.1.3. Relative control function

Since the controlled degrees of freedom are uncoupled a simple non linear impulsive control is used: the dead band control allows to maximize the time between consecutive pulses while guaranteeing to stay inside the control box. The movement consists of a parabola going from the lower to the upper control bound, the relative trajectory is thus always inside a corridor whose width is tunable depending on the mission phase. An example of the position control error is given on the following figure for a 4-day observation (which is not necessarily realistic since no observation will be made during perigee passes). The thrust is applied against the perturbation whose magnitude is provided by the relative navigation function. Apart from the estimation error, the limitation on relative control performances comes from the pulse resolution. Without taking into account the estimation errors nor the actuation errors, the global delta-V budget for a fine relative

position control over one orbit is about 0.02m/s, only counteracting the gravity gradient and the solar pressure differences between the two spacecrafts. The control frequency is low: a pulse every few hundreds of seconds in the worst case.

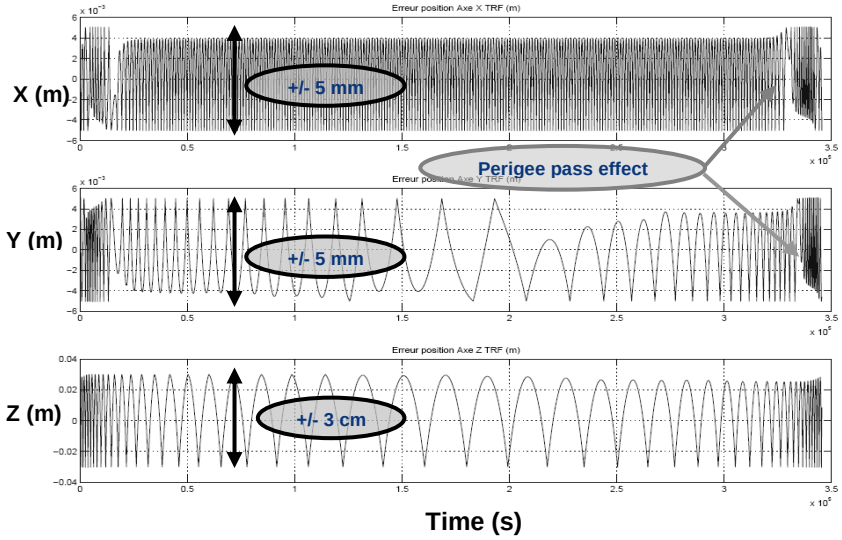

Fig. 6 Relative position error in an inertial frame during 4 days

2.1.4. Relative guidance function

The Rendezvous algorithm involved in the Homing sub-phases of the Formation Acquisition sequence, is based on 3 elements:

- a relative dynamics model, which enables to perform an integration of the motion and propagate the relative state at the chosen date. This model outputs also the manoeuvres needed to reach the target state.

- an optimization method, that uses the relative dynamics to evaluate the velocity increments to perform the requested Rendezvous.

- a method to plan Rendezvous scenarii, that constraints the parameters of the optimization method in order to guarantee a robust behaviour of the overall Rendezvous.

For operational reasons it is needed to have a relative guidance function as autonomous as possible. The ground/board sharing between the previously introduced functionalities shall thus take this aspect into account. Regarding the relative motion integration and the maneuver re-computation the driving need is to have a control with short reaction times, thus the functionality is set on-board. As far as the planification method is concerned, it is not possible to build an autonomous planification method robust enough to cope with all possible configurations, namely in

terms of orbital positions, transfer durations or ISD. This is the reason why this part is intended to remain on ground. For the optimisation part, different methods are possible. It is interesting to select a simple method, in case it is chosen to be implemented on-board. Once this method is fixed the planification principle shall be adapted to the chosen optimisation method in order to guarantee robustness.

Four different models of relative dynamics are considered today and listed below:

- Clohessy-Wiltshire model
- Lawden model
- Yamanaka-Ankersen model
- Differential keplerian elements model

Two different optimization methods are considered

- Least square method
- Simplex method

To each of these methods correspond a dedicated planification strategy :

- Planification of the maneuver dates for the least square method
- Planification of the computation step and the number of maneuvers for simplex method

For a first evaluation of the guidance strategy and with regard to the navigation errors, Clohessy-Wiltshire [2] model was used for the simulation presented below eventhough Yamanaka-Ankersen [4] model seems the best suited to the HEO context. The optimization function relies on a least square method and a planification that fixes the manœuvre dates.

The Rendezvous algorithm has been designed to work with the onboard estimated relative state and a pre-defined manoeuvre plan $\{t_k, \Delta V_k\}$ (with k $\leq$10). An initial manoeuvres plan is uploaded by telecommand and the on-board algorithm updates autonomously this plan with respect to the current estimated relative state $X(t)$ with the objective to get to the target $X(t_c)$ on time t_c and without changing the dates of manoeuvres.

For a Rendezvous from 30 km to 500 m with a 50000 s fixed duration, the following assumptions are made:

- at the starting date of the Homing phase the MSC is at the apogee and the DSC is 30 km far from the MSC on the velocity axis,
- at the end of the Homing phase the target state for the DSC is at 500 m on the MSC velocity axis,

The target state (position and velocity) is reached with the following accuracy in m and m/s without taking into account any perturbation:

$X_{realized} - X_{target} = (0.00004, -0.00084, 0., 0.00001, 0.00002, 0.)$ in a (T,N,W) frame. This result is reached with a total propellant consumption of $C = \sqrt{\left(\sum|\Delta V_{t,i}|\right)^2 + \left(\sum|\Delta V_{n,i}|\right)^2 + \left(\sum|\Delta V_{W,i}|\right)^2} = 1.60044\ m.s^{-1}$

2.2. Absolute attitude concerns

2.2.1. Guidance

During formation flying phases, the required performance on FFRF sensor outputs implies some constraints on the attitude configuration.

During an observation, the telescope line-of-sight is perpendicular to the sun direction ±20°. Even though both spacecrafts have fixed solar arrays, this configuration prevents from any constraints on power management during Mission phase. Regarding Retargeting phases, there are short enough not to take into account any power constraint either. For the Formation Acquisition phase that takes place around the apogee and lasts around 24 hours, the trade-off between FFRF sensor configuration and power constraints is not that obvious. Indeed FFRF sensor measurements accuracy is dependent on the relative attitude between the triplet antenna plane normal direction and the LOS. During IAR the Detector satellite reference frame shall be aligned with LOS and solar arrays depointing w.r.t the Sun shall stay below 45°.

Once the IAR has been performed, the angle between the satellite frame and the LOS shall be lower than 20° in order to keep a few degrees of accuracy on the LOS measurement. On the other hand solar arrays depointing w.r.t the Sun shall remain below 45°.

The global (pre-acquisition and acquisition) sequence corresponds to a time window being opened by the 45° constraint, and closed by the 65° constraint. This time window is computed over the 2014-2019 period, and takes into account all perturbations and also a typical set of Station keeping manoeuvres. The reference ephemeris of the satellites are used for the simulation.

These values, obtained theoretically and in the keplerian case, have to be consolidated by the means of simulations taking into account all perturbations and uncertainties. The time slot is defined according to the following aspects:

- the whole slot must take place at less than 36 hours from the apogee (one day is avoided around the perigee)
- the slot is opened as soon as the Sun angle w.r.t. the plane normal to the velocity vector (which represents the reachable direction for the normal to the solar pannel) is lower than

45°. This is the condition to start the pre-acquisition phase (the Satellite reference frame can be aligned with the LOS).

- the slot is closed when the Sun angle w.r.t. the plane normal to the velocity vector becomes higher than 65°. This represents the latest time when a configuration close to the final Formation Flying has to be reached.

The simulation result is illustrated by the following graph:

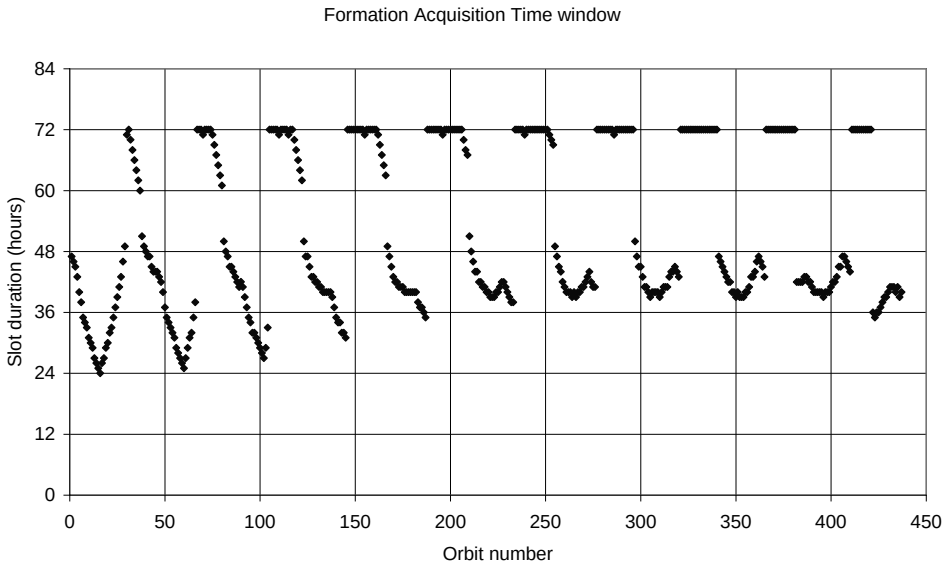

Fig. 7 Formation Acquisition time window

On all 440 orbits of 2014-2019 time period there is always a slot of at least 24h where both the Sun and the 20° LOS constraints are met. The lowest durations for the slot (24 hours) occur at beginning of life. Indeed, since the orbit inclination is still low, the Sun remains close to the orbital plane (the Sun aspect angle does not get very high), which corresponds to a worst case. An autonomous attitude guidance algorithm taking into account these constraints is thus feasible in the sense that a solution always exits.

2.2.2. Control

For SIMBOL-X mission there is no need to have a relative attitude control. Each spacecraft is controlled independently and the absolute attitude control accuracy combined with the relative position control accuracy guarantees that mission requirements are met. Following feasibility phase studies, a trade-off between continuous attitude control (using reaction wheels) and impulsive attitude control (using cold gas) has been performed: the impulsive control solution may offer advantages for the LOS reconstruction (pixel noise filtering) but the continuous control solution is

still under evaluation at this stage of the project. The method used for impulsive attitude control is the same as for relative positioning control. System requirements demand an absolute 2-arcmin pointing accuracy for Detector spacecraft.

3. LOS CONTROL AND RESTITUTION

Top-level scientific requirements involve different aspects : besides the instrument static performances some of these requirements directly constraint GNC performances. The more stringent requirement as far as GNC is concerned is the a posteriori LOS restitution in an inertial frame within 3as accuracy. This LOS reconstruction through GNC outputs, implies the elaboration of a very strict budget regarding all the GNC error contributors. But other scientific requirements have also an impact on the GNC design. This last section will thus introduce the different links between scientific requirements and GNC design. Once those links have been established and the constraints have been highlighted, focus will be made on the chosen methodology to make a first LOS budget. A full 3D LOS expression gives the complex coupling between the various degrees of freedom and the effect of each GNC error source. This analytical analysis shall be consistent with further simulation results.

3.1. Scientific requirements and LOS budget

During the mission the expected photon flux is very low for most of the observed sources. Each detected photon is recorded in the mass memory with its detection date, its position in the detector array and its energy. These records represent the scientific telemetry, which is downloaded to the ground at each perigee pass (every 4 days), together with the satellites sensors measurements.

3.1.1. Field of view (FOV) and LOS control

The required FOV is 12 arcmin. This corresponds to a 7 cm detector diameter at 20 m in a static configuration. The SIMBOL-X field of view is the result of the combination of the static instrument field of view and of the formation flying dynamics (lateral relative motion of the satellites; detector tilt effect is negligible). The figure below illustrates the effect of the relative lateral motion on the field of view. The smallest circle is the mirror FOV projection in the focal plane. When the focal plane moves laterally this projection is no longer centred. In order to keep the FOV inside the detector plane, the detector focal plane must be wider than the mirror FOV. In fact its size must cover the mirror FOV plus the formation flying lateral tolerance.

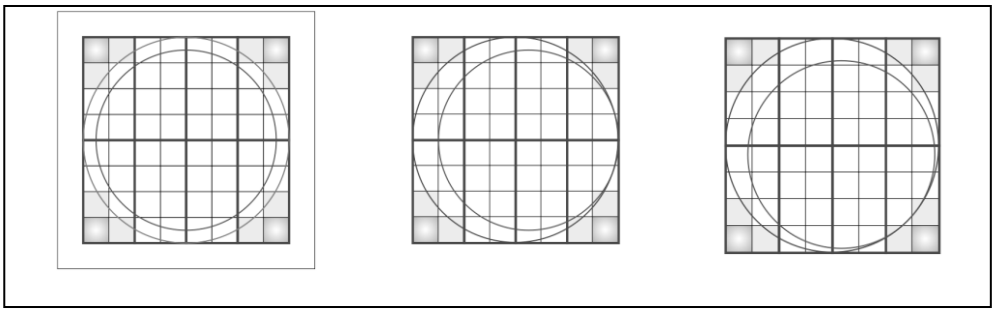

Fig. 8 FOV tolerance on lateral motion

An increase of the detector diameter would be a first solution but mass and consumption shall be reduced as much as possible. Another constraint stems from the reuse of an existing Low Energy Detector (LED) design. This LED has a maximal diameter of 8 cm (around 13.75 arcmin at 20 m)

The resulting formation flying tolerance is thus of +/- 5 mm at a 20-meter intersatellite distance which corresponds directly to the relative position control performance requirement during mission phases on lateral axis.

3.1.2. Angular resolution, absolute pointing and LOS restitution

The image corresponding to an observation is reconstructed on ground by translating each photon accordingly to the estimated LOS at the time of its detection. Thus the LOS estimation, or reconstruction, is of primary importance for the mission performances. Hereafter, this effect is illustrated with the case of a point source.

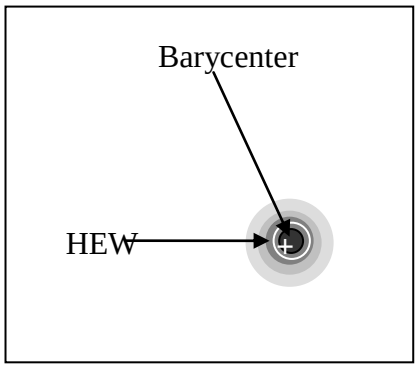

Image of a point source (PSF) for a perfectly pointed telescope (not representative of a real mirror)

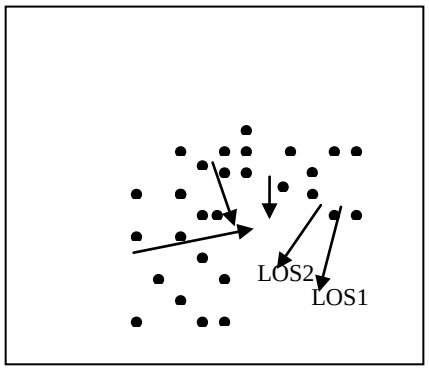

Simbol-X raw data for a point source – Detection are spread in the detector because of the relative dynamics
On ground, each photon position is corrected using the reconstructed LOS

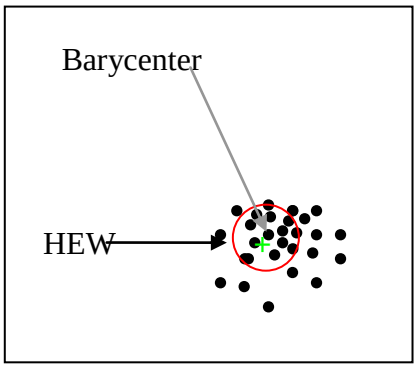

Simbol-X point source reconstructed image – The LOS error distribution impacts the image quality

Fig. 9 Image reconstruction

The angular resolution is specified at 20 arcsec HEW (Half Energy Width) for 30 keV energy sources. This can be interpreted in terms of probability on the photons reconstructed positions for a punctual source. In particular we have $P(r_{photon} < 20") = 0.5$, where r_{photon} stands for the radial distance between the photon detection point and the source barycentre in the detector.

The final angular resolution is the combination of the static instrument angular resolution and of the noise on the LOS knowledge at the frequency of the photon arrival (which is assumed to be at maximum 100 Hz). We assume Gaussian distribution for both contributors, noting $\sigma_{Instrument}$ and σ_{LOS} their respective rms. As they are independent, the resulting angular resolution may be written $\sigma = \sqrt{\sigma_{Instrument}^{2} + \sigma_{LOS}^{2}}$.

Considering the current state-of-art technology on mirror, and taking some margins the following allocation is chosen: $\sigma_{Instrument}$ =15" and σ_{LOS} =4" for the LOS restitution noise.

3.1.4. Absolute pointing accuracy

The requirement regarding the absolute pointing accuracy is of 3 arcsec (goal 2 arcsec) (90%). It is the accuracy of the reconstruction of the sources absolute position on the vault. The last requirement is applicable whatever the source in the field of view. This position is computed from the source image barycentre estimated position in the focal plane and from the distributed instrument estimated line-of-sight during the observation as already explained above.

Therefore the achievable performance depends on the instrument barycentering performance (including the instrument performance itself and the barycentering algorithms efficiency) and on the LOS reconstruction accuracy. The barycentering performance is linked to the algorithms used and to the pixel size.

Concerning the LOS contribution, the error on absolute pointing comes from the bias, which is, for a given observation, the value of the bias itself, and which impacts all the sources in the field of view.

The LOS bias is the result of the combination of different biases all along the LOS metrology chain. This bias may be partially corrected by calibration on well-known sources. However the calibration process is not perfect (knowledge of calibration sources positions, barycentering…) and leads to bias residual. Furthermore, the calibrations are not performed using the same sources as the one targeted for mission purposes, which may lead to a different bias between the calibrated one and the real one during an observation: a bias stability term shall be evaluated in the LOS budget too.

The overall error on absolute pointing is therefore the sum of three main physical contributors:

- bias stability that corresponds to metrology FOV and thermoelastic effects

- bias residual after calibrations
- barycentering error

The initial scientific requirement is thus decomposed in the following way:

- barycentering error shall be less than 0.6” (goal 0.5”) (3σ)
- bias stability shall be within 2” (goal 1.5”) (3σ)

One can notice that the barycentering performance is involved twice, at the sources position computation in the focal plane level and at the LOS bias calibration level. In the same way the thermoelastic and FOV effects are also indirectly involved in the bias residual.

3.2. Line-of-sight analytical analysis

As shown before, the LOS reconstruction performances are of primary importance for final instrument performances. More precisely :

- the reconstructed LOS stability over the observation impacts the final instrument Point Spread Function (PSF)
- the reconstructed LOS mean accuracy over an observation impacts the instrument astrometry performance, that is to say the accuracy of the absolute localisation of observed sources in the instrument field of view

Those two aspects can not be evaluated at the same frequency range. In order to be as exhaustive as possible and without making any assumptions on the LOS error function frequential signature, a first analytical analysis is performed in order to obtain the equation of SIMBOL-X line-of-sight in 3 dimensions including all the possible macroscopic uncertainties. The proposed approach does not assume any conception choice (except the use of star tracker on each platform and the use of an optical sensor including a target to perform accurate lateral measurements).

The instantaneous error function to be characterized is the difference between the reconstructed LOS and the actual LOS. As illustrated on the figure below, this reconstruction will be processed on ground based on information output by:

- the star trackers mounted on the DSC (STR_D) and on the MSC (STR_M)
- the optical sensor mounted on the DSC (point B) and aiming an optical target mounted on the MSC (point K)

Some other major information will come from the knowledge of the geometry and the architecture of the platforms.

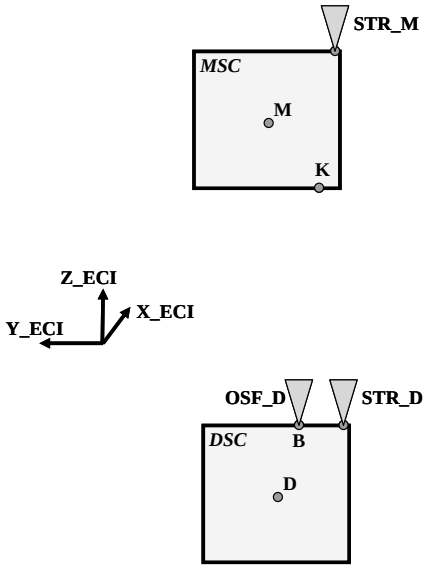

Fig. 1: Line-of-sight schematics

Each equipment outputs its measurements in particular frames that are defined in the following table:

Table 1: Frames definition

Notation	Definition	Comments
ECI	Earth Centred Inertial	Reference inertial frame in which the LOS reconstruction shall be processed
ORF_M	Optical Reference Frame on Mirror S/C	Frame related to the mirror module
ORF_D	Detector Reference Frame on Detector S/C	Frame related to the detector payload
STR_M	Star Tracker on Mirror S/C	Measurement frame for the STR mounted on the MSC. In case of multi heads STR, a mean (barycentre) frame is considered.
STR_D	Star Tracker on Detector S/C	Measurement frame for the STR mounted on the DSC. In case of multi heads STR, a mean (barycentre) frame is considered.
OSF_D	Optical Sensor Frame on Detector S/C	Measurement frame of the lateral sensor.

The different error sources that are identified in this approach are listed thereafter:

- uncertainty about the distance between 2 points of a body (initial uncertainty, thermo elastic deformation…) ε
- distance measurement error: optical sensor measure δ
- uncertainty about the alignment between 2 frames α
- orientation measurement error: star tracker or optical sensor measure (on 1 axis) β

Besides, to correctly carry out the calculus and to lighten the equations some assumptions are taken:

- the real line-of-sight is aligned with Z_ECI. The LOS norm is f, the SIMBOL-X focal length

- X, Y and Z axis of the star tracker and optical sensor are nominally merged with the X, Y and Z axis of the spacecraft frame on which they are mounted. This is a sort of reference orientation which facilitates the calculus and does not restrict the problem. Of course the true misalignments are taken into account in the calculus
- the rotations considered in this study are of small amplitude (< 1°). They are described with the Euler angles. The considered rotations originate from thermo elastic deformation (a few arcsec) and DSC depointing with respect to the inertial frame (< 1°)
- the distance measurement error δ (optical sensor measure) can be identically reported along the BK vector. It is naturally the case if the distance measurement is provided by the optical sensor
- the optical centres (D, M) of the spacecraft can be merged with their centres of gravity. This assumption simplifies greatly the computation. In reality, the rotations will be performed around the gravity centres, which leads to a rotation of the DB and KM vectors (correctly modelled), combined with a translation of these vectors. This translation induces a modification of the real LOS with respect to the reference LOS, and this modification is covered by the first assumption
- the BK vector is mainly along Z axis. Its component along X and Y can be neglected in the computation of its norm with respect to the Z component

Using the introduced notation, the real line-of-sight vector can be decomposed over three vectors:

$$DM_{r,ECI} = DB_{r,ECI} + BK_{r,ECI} + KM_{r,ECI}$$

With DB being the vector linking DSC optical centre to the optical head of the lateral sensor on DSC.

BK being the vector linking the optical head of the lateral sensor to the target of the lateral sensor on MSC.

KM being the vector linking the target of the lateral sensor (MSC) to the MSC optical centre.

As for the real vector, the measured LOS vector can be decomposed over three other vectors that are the measured ones:

$$DM_{m,ECI} = DB_{m,ECI} + BK_{m,ECI} + KM_{m,ECI}$$

From the previous developments it is possible to get the error on the instantaneous LOS measurement:

$$xLOS\_error = ux.\left\{DM_{m,ECI} / (f + \delta_{BK}) - DM_{r,ECI} / f\right\}$$

$$yLOS\_error = uy.\left\{DM_{m,ECI} / (f + \delta_{BK}) - DM_{r,ECI} / f\right\}$$

With *u* the unitary LOS vector expressed in ECI.

A full development of the last two equations is performed and used in order to get a physical understanding of the problem. The list of contributors is thus identified, alongside with their multiplying factor.. The analytical contribution of the main sources, issued from the full 3-D equation development, is given below:

$\left(\frac{z_{BK}}{f}+\frac{z_{DB}}{f}\right)\beta_{STR\_D\_y}\Rightarrow$ STR_D error around transverse axes

$\left(-\frac{y_{KM}\beta_{STR\_M\_z}}{f}\right)\Rightarrow$ STR_M error around its line-of-sight

$\left(\frac{z_{BK}\beta_{OS\_y}}{f}\right)\Rightarrow$ optical sensor direct error

$\left(\frac{y_{BK}\alpha_{D\_2\_z}}{f}-\frac{z_{BK}\alpha_{D\_2\_y}}{f}\right)\Rightarrow$ misalignment between STR_D and optical sensor OSF_D

This analytical approach is now used to highlight the key factors and/or the negligible ones in the instantaneous error budget .The global error sources analysis is synthesised in the next table for the x component of the line-of-sight. The same analysis can be made for the y component. Typical orders of magnitude are provided for each error source together with a typical amplification factor. These figures must be manipulated with extreme care since they do not constitute a precise error budget, but rather the contribution of each error in the global instantaneous budget. The idea is rather to highlight the key factors of the LOS error sources and emphasize some critical error sources which shall not be neglected.

Table 2: LOS error main contributors on x component

Contributor on x component	Amplifying factor	Orders of magnitude of resulting contribution
DSC star tracker error wrt LOS	1	1 as
Optical metrology lateral error	1	1 as
Misalignment between DSC star tracker and optical sensor	1	1 as
DSC star tracker error around LOS	~0.4/20	~0,1 as
MSC star tracker error around LOS	~0.4/20	~1 as
MSC star tracker error wrt LOS	~0.4/20	~0,1 as
Misalignment between detector payload and DSC star tracker	~0.5/20	~0,02 as
Misalignment between mirror and MSC star tracker	~0.5/20	~0,02 as
Elongation between detector payload and optical sensor	~1/20 m^{-1}	~0,01 as
Elongation between mirror et optical sensor target	~1/20 m^{-1}	~0,01 as
Distance measure error	~2,5.10^{-4}	~0,5 as

Now that key factors have been highlighted, a method shall be chosen in order to evaluate the real contribution of each factors on the angular resolution and on the absolute pointing accuracy. The decomposition and combination of the error sources are adapted from ECSS (European Cooperation for Space Standardization) recommendations. The main principles are:

- the LOS error computation is done separately for x and y axis (in the Satellite reference Frame)
- errors are decomposed in frequency classes and characterized (here by a rms value)
- in each frequency class, the different contributions are weighted by the relevant factor from the LOS equation and combined (quadratically if independent, linearly if dependent)
- the resulting contribution of the frequency classes are combined together
- the obtained x and y axis error are combined (quadratically)

As exposed previously around 1000 different sources will be targeted during the mission. A random distribution of the pointing on the celestial vault shall thus be considered in the LOS error budget computation.

The following frequency classes have been identified :

- constant over the mission: constant bias
- constant over an observation: the error is constant during an observation (therefore it is seen like a bias). It may change from one observation to another (FOV and thermoelastic effects)
- low frequency over an observation: the error changes during an observation with a typical period from about 10s up to a few thousands seconds. Its average value over one observation is null (pixel errors)
- high frequency: the error changes with a typical period of less than a few seconds. Its average value over one observation is null

The LOS stability budget involves contributions which exhibits variations over an observation with a null mean value. By definition these are the "Low frequency over an observation" and the "High frequency" classes. The final LOS stability budget is obtained using the principles exposed above.

The LOS astrometric budget involves contributions which have a non-null mean value over an observation. By definition these are the "Constant over the mission" and the "Constant over an observation" classes. The summation rules are slightly different from what exposed above. The chosen computation procedure is the following one:

- the cumulated constant bias is calibrated periodically in flight. Only the calibration residual is considered for the budget
- for the "constant over an observation" frequency, each error source shall be characterized (by a rms value) axis by axis in the Satellite Reference Frame. This rms value shall be estimated over the entire set of pointing
- each contribution shall then be multiplied by the relevant factor, respectively for the x and y LOS components
- for each of the x and y axis, contributors are combined. Combination rules state that independent contributions should be summed quadratically and dependent ones linearly.
- the final LOS astrometric budget is obtained by quadratic summation of LOS x and LOS y error, further added to the calibration residual

According to ECSS standards, the calibration residual should be combined quadratically to the other contributors. However, considering the relatively low number of calibrations, a linear sum seems more appropriate.

4. CONCLUSION AND PERSPECTIVES

SIMBOL-X represents the first operational mission using formation flying techniques. Beginning of 2009 the project will enter its preliminary definition phase. During this phase the system architecture shall be frozen and the preliminary GNC technical solutions, lately exposed, shall be completely defined.

Regarding formation flying and Rendezvous algorithms, the launch of PRISMA formation flying demonstrator next year and its experiments evaluation shall offer very interesting inputs. In particular the PRISMA/FFIORD experiment [6] will be of prime interest for SIMBOL-X mission enabling an extensive use of FFRF metrology and GNC algorithms (navigation function, Rendezvous guidance function). Many other challenges need yet to be undertaken by SIMBOL-X mission due to the context differences (HEO orbit, stringer requirements, use of a new metrology, LOS restitution…).

As far as the LOS problematic is concerned a simulation tool is being developed in tight cooperation with the scientific laboratories. This Matlab/Simulink simulator is an engineering tool intending to :

- characterize the degradation of the image due to the different LOS error contributors and better understand the scientific needs
- characterize the LOS error itself, in order to consolidate the first theoretical analysis on the key contributors and to provide statistical figures to affine the system requirement allocation
- compare the LOS error contributors with some other contributors such as the PSF or the focal plane geometry.

References

1. Berge S. and Al, “Rendezvous and formation flying experiments within the PRISMA in-orbit testbed”, 6th International ESA conference on GNC, 2005
2. Clohessy W. and Wiltshire R., “Terminal Guidance System for Satellite Rendezvous“, Journal of the Aerospace Sciences, vol. 27, No 9, 1960, pp 653-658, 674
3. Berges J.C and Al, ”CNES approaching guidance experiment within FFIORD”. 10th International Symposium on Space Flight Dynamics - September 24-28, 2007 Annapolis, Maryland.

4. Yamanaka K. and Ankersen F., “New state transition matrix for relative motion on an arbitrary elliptical orbit”, Journal of Guidance, Control, and Dynamics, vol.25, no.1, 2002, pp 60-66
5. Blare L. and Al., “A lateral Sensor for SIMBOL-X derived from Hydra Star Tracker”, 3rd International Symposium on Formation Flying, Missions and Technologies, 2008, Noordwijk
6. Delpech M. and Al., “FFIORD experiment on PRISMA - GNC validation, test and performance”, 5th Workshop on constellations and formation flying, 2008, Evpatoria
7. R. Cledassou and P. Ferrando ,"SIMBOL-X: An hard X-ray formation flying mission", Workshop "Focussing telescopes in nuclear astrophysics", 2006

Authors

P. Y Guidotti, CNES, 18 av Edouard Belin, 31041 Toulouse (France)
Contacts: pierre-yves.guidotti@cnes.fr
M. Delpech, CNES, 18 av Edouard Belin, 31041 Toulouse (France)
S. Djalal, CNES, 18 av Edouard Belin, 31041 Toulouse (France)
A. Gaudel-Vacaresse, CNES, 18 av Edouard Belin, 31041 Toulouse (France)
J. C. Berges, CNES, 18 av Edouard Belin, 31041 Toulouse (France)
P. Gamet, CNES, 18 av Edouard Belin, 31041 Toulouse (France)
Olivier La Marle, CNES, 18 av Edouard Belin, 31041 Toulouse (France)